IEEE Access
Multidisciplinary | Rapid Review | Open Access Journal

Received May 23, 2021, accepted June 4, 2021, date of publication June 8, 2021, date of current version June 16, 2021.

Digital Object Identifier 10.1109/ACCESS.2021.3087513

Realization of a Wideband Series-Fed 4 × 4-Element Waveguide Slot Array in the X-Band

JIYU HE[1], YAXIANG WU[1], (Graduate Student Member, IEEE), DAN CHEN[1], MIAO ZHANG[1], (Senior Member, IEEE), JIRO HIROKAWA[2,1], (Fellow, IEEE), AND QINGHUO LIU[3], (Fellow, IEEE)

[1]Institute of Electromagnetics and Acoustics, Xiamen University, Xiamen 361005, China
[2]Department of Electrical and Electronic Engineering, Tokyo Institute of Technology, Tokyo 152-8552, Japan
[3]Department of Electrical and Computer Engineering, Duke University, Durham, NC 27708, USA

Corresponding author: Miao Zhang (miao@xmu.edu.cn)

This work was supported in part by the National Natural Science Foundation of China under Grant 61971364, and in part by the Natural Science Foundation of Fujian Province, China, under Grant 2017J01122.

ABSTRACT The series-fed subarray still plays a critical role in a partially-corporate-fed array, which has advantages over the corporate feed one in terms of both beam steerability and freedom in array sizes. In this paper, two techniques are presented for the wideband design of series-fed waveguide slot arrays. Firstly, the overload technique is adopted to design standing-wave fed 1 × 4-element arrays of both coupling slots and radiating slots. The simulated bandwidths for $|S_{11}| < -15$ dB are enhanced to 8.1% and 12.2%, respectively. Secondly, the open-cavities, namely decoupling structures above radiating slots, are introduced to suppress the mutual couplings among a 4 × 4-element array. Its bandwidth for $|S_{11}| < -15$ dB is significantly improved from 5.1% to 11.3%. For demonstration, a 4 × 4-element array is designed in the X-band, and is fabricated by Direct Metal Laser Sintering technique. The measured bandwidths for $|S_{11}| < -12.5$ dB and the antenna efficiency higher than 70% are as wide as 12.4% and 9.5%, respectively. The validity of those wideband design techniques is verified.

INDEX TERMS Waveguide slot array, wideband design, standing-wave feed, overload technique, decoupling structure.

I. INTRODUCTION

The waveguide slot array is characterized by the low profile, high-power capacity, low loss, and high efficiency even in the millimeter-wave (MMW) band. It has been widely applied for space, radar, and wireless communications for decades. However, its limited bandwidth of less than 5% is well known as one major drawback. In recent years, the high-gain and wideband array antennas have attracted significant attention from high-resolution radar and high-capacity wireless communication systems. Conventionally, wide slots and dumbbell slots [1]–[3] have been adopted to improve the overall bandwidth of a waveguide slot array. However, those approaches are unsatisfactory, and the corresponding antenna performance regarding cross-polarization discrimination (XPD) would be degraded as a tradeoff.

The associate editor coordinating the review of this manuscript and approving it for publication was Bilal Khawaja.

One effective way to improve the antenna bandwidth is to decompose the overall array into several subarrays. When the feeding circuits evolve from the series-fed structure into the center-fed, partially-corporate-fed, and corporate-fed structures, the corresponding bandwidths are significantly enhanced by reducing the long-line effects [4]–[13]. Over the last decade, the corporate feed becomes dominant in realizing a wideband high-gain beam-fixed array, whose number of elements in one dimension is generally restricted to 2^N instead of an arbitrary integer. For example, the corporate-fed slot arrays based on the conventional hollow waveguide technique [14]–[19] and the ridge gap waveguide technique [20]–[22] have been successfully developed in the MMW band. Meanwhile, various corporate-fed slot arrays based on the dielectric-filled post-wall waveguide and substrate integrated waveguide (SIW) have been studied for MMW applications [23]–[25]. All of those corporate-fed array antennas

adopt the double-layer cavity-backed structures associating with a 2 × 2-element subarray as the radiating unit.

On the other hand, the partially corporate feed still has advantages over the corporate feed in terms of both beam steerability and freedom in array sizes. It has broader applications in SAR (Synthetic Aperture Radar) and wireless communication systems. As an assumption, a 16 × 16-element array is under development. By replacing the center feed with the partially corporate feed, the overall array can be decomposed into 8 × 8- and 4 × 4-element end-feed subarrays. Then, the number of in-series elements can be reduced from 8 to 4 and 2, respectively. In this way, the overall array bandwidth can be doubled and quadrupled straightforwardly. Moreover, the overall array design is also simplified into the designs of subarray and feeding network. Therefore, the wideband design of a subarray becomes essential.

A technique called "overload" [3], [26] has been introduced in the design of a one-dimensional (1-D) standing-wave fed array to expand its matching bandwidth effectively. By overloading the slotted waveguide, the matching bandwidth of the 4-element subarray was improved to about 9.5% for VSWR < 1.5. However, when applying this overload technique to designing two-dimensional (2-D) arrays, the matching bandwidth of the center-fed 8 × 10-element array [10] was improved to only 4.5% for VSWR < 1.5. The effect of bandwidth enhancement in a 2-D array is limited compared with that in a 1-D array. Therefore, the mutual coupling among slots may seriously defect the overload technique and degrade overall bandwidth performance.

Previously the baffles as well as open-cavities, functioning as the decoupling structures, have been introduced in the external region of radiating slots [15], [27]–[30]. The decoupling becomes essential when designing a high-performance 2-D array in terms of aperture distribution, radiation pattern, and impedance matching. As illustrated in [30], when the mutual couplings among radiating slots are effectively suppressed by optimizing the three-dimensional (3-D) sizes of open-cavities, the active admittance of a slot lying in a 2-D array is identical to its own self-admittance. Hence, one slot even belonging to a 2-D array may operate as if it exists alone.

In this paper, a 4 × 4-element waveguide slot array, which can be widely adopted as a subarray to realizing a high-gain array with a fixed or scanned beam, is demonstratively designed and tested for wideband operation in the X-band. Firstly, we apply the overload technique to improve the bandwidths of standing-wave fed 1 × 4-element subarrays. The performance for both coupling slots and radiating slots is examined. Secondly, the effects of mutual couplings among radiating slots are investigated in detail. Thirdly, under the periodic boundary condition, the decoupling structures, "open-cavities," is additionally introduced in the 1 × 4-element subarray, and effectively improves its bandwidth. Forthly, we combine the subarrays of radiating and feeding parts into a 4 × 4-element array. Under the conditions of both radiation and periodic boundaries,

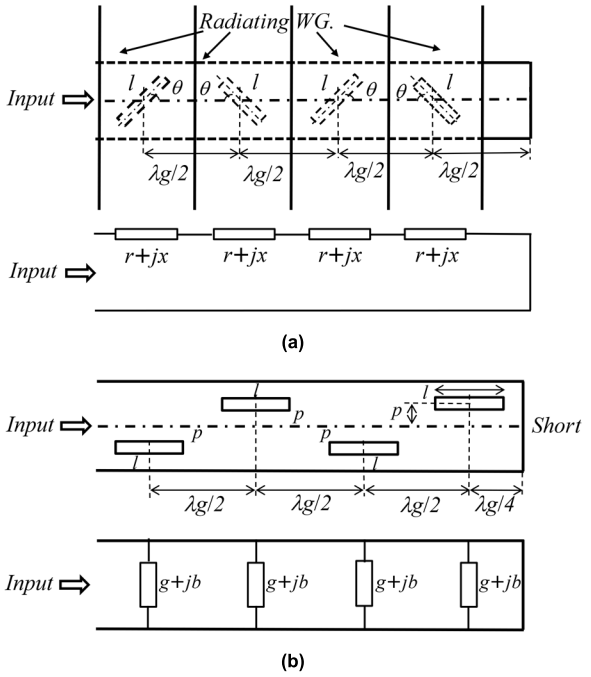

FIGURE 1. Series-fed waveguide slot arrays and their equivalent circuits. (a) 1 × 4-element subarray of coupling slots and its equivalent circuit; (b) 1 × 4-element subarray of radiating slots and its equivalent circuit.

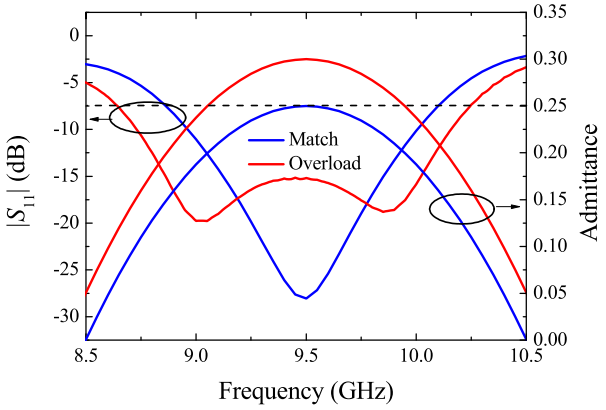

FIGURE 2. Principles of match and overload design technique.

the bandwidth improvement is observed when introducing open-cavities. Finally, we fabricate the 4 × 4-element array by the DMLS (Direct Metal Laser Sintering) technique. After experimental evaluations, the validity of those wideband design techniques is verified.

II. OVERLOAD TECHNIQUE

Fig. 1 illustrates the series-fed waveguide slot arrays and their equivalent circuits. In this study, the center-inclined slots and longitudinal slots are adopted as the couplers and radiators, respectively. It is well-known that their equivalent circuits are respectively represented by four impedances in series and four admittance in parallel, as shown in Fig. 1. The element spacing for both coupling and radiating slots is fixed at half

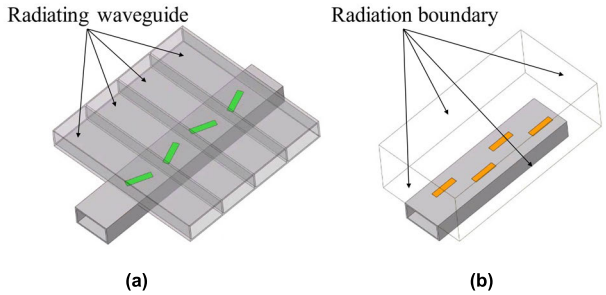

FIGURE 3. Simulation models of 1 × 4-element subarrays. (a) Feeding part. (b) Radiating part.

TABLE 1. Slot parameters and bandwidths of 1 × 4 coupling slots for different designs.

Design	I	II	III
$\|S_{11}\|$ @ 9.5GHz (dB)	-10	-15	-20
Slot length l (mm)	14.70	14.80	14.85
Slot angle θ (deg.)	22.40	19.30	17.8
Matching Bandwidth (%)	11.3	8.1	5.9

a guided wavelength in common. The FEM-based (Finite Element Method) high-frequency electromagnetic-field simulator Ansys HFSS is applied to the array analysis and design.

According to our investigation, the standing-wave-fed array exhibits larger matching bandwidth than the traveling-wave-fed one when the number of in-series elements is sufficiently small [11]. Generally, to achieve perfect matching at the center frequency, the structural parameters are optimized to realize a normalized input impedance or admittance equal to 1. For simplicity, identical structural parameters are assumed for the four slots in series. Hence, the normalized impedance or admittance of a single slot is just 1/4 in the 1 × 4-element subarray. The reflection and admittance are diagrammatically drawn as a function of frequency. As shown in Fig. 2, the principles of "match" and "overload" are respectively illustrated by blue and red lines for comparison. The reflection of the matched subarray exhibits a single resonance.

For wideband operation, the overload technique is introduced further to enhance the matching bandwidth of a standing-wave-fed array. When the impedance or admittance of each slot is uniformly enlarged from 1/4 to some extent at the center frequency, the slotted waveguide is overloaded, i.e., the normalized input impedance or admittance is larger than 1. On the other hand, it approaches 1 at the lower and higher frequencies, according to the frequency behavior of impedance or admittance, as illustrated in Fig. 2. That is, a double-resonance behavior is achieved over the operating frequency range. Therefore, the matching bandwidth is significantly enhanced by applying the overload technique for a specific $|S_{11}|$.

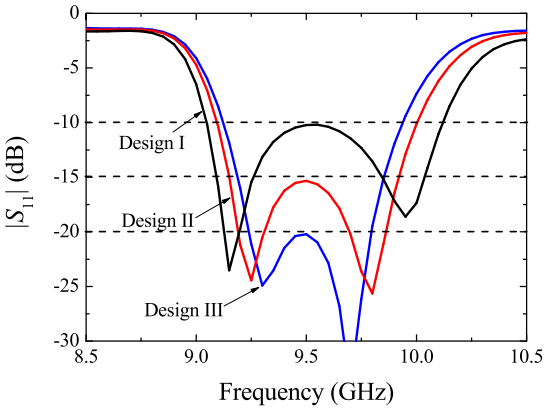

FIGURE 4. Reflection coefficient $|S_{11}|$ of 1 × 4 coupling slots for different designs.

III. WIDEBAND DESIGN OF 1 × 4 COUPLING SLOTS

In the feeding part, the 1 × 4-element subarray of coupling slots is designed by applying the overload technique first. Its simulation model in HFSS is shown in Fig. 3 (a), where the coupling slots are isolated in the external region. The upper radiating waveguides adopt the standard waveguide WR-90 with a cross-section of 22.86 mm × 10.16 mm, while the lower feeding waveguide has a cross-section of 21.05 mm × 10.16 mm. They couple through the center-inclined slots with a spacing of half-guided wavelength. As the key structural parameter, the tilt angle θ and length l of a center-inclined slot cut in a rectangular waveguide mainly control the equivalent resistance r and reactance x, respectively. During the subarray design, a single resonance is first observed in the frequency characteristics of reflections when the angle θ is less than a specific value. If the slot angle θ is continuously increased, a phenomenon of double resonance rather than single resonance is observed and exhibits a wider matching bandwidth for a certain $|S_{11}|$.

Three types of 1 × 4-element subarrays are designed for comparison. The worst values of reflection coefficient ($|S_{11}|$) at the center frequency are set at −10, −15, and −20 dB, respectively. As listed in Table 1, the parameters of θ and l are mainly optimized to satisfy different design criteria. As the design bandwidths for $|S_{11}| < -10$, −15, and −20 dB are achieved as 11.3%, 8.1% and 5.9% respectively. By increasing the tilt angle θ, the slotted feeding waveguide is overloaded, and the matching bandwidth is enhanced. However, as a tradeoff, the impedance matching at the neighborhood of center frequency degrades to some extent. By the way, compared to the matched subarray with a single resonance, the matching bandwidth for $|S_{11}| < -15$ dB is improved by 2.7%.

During the abovementioned subarray design, the feeding waveguide height b and the slot width w are fixed at 10.16 mm and 3.6 mm, respectively. According to our investigation, those two parameters also exert a non-negligible influence on the matching bandwidth. Its dependence on those two parameters is studied in detail. For a fixed b or w, θ and

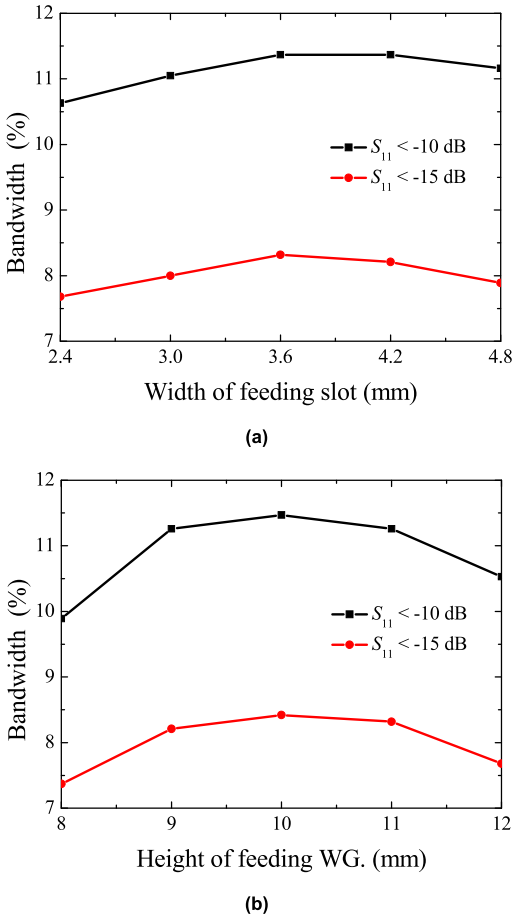

FIGURE 5. Bandwidth dependence on other parameters. (a) Dependence on widths of feeding slot. (b) Dependence on height of feeding waveguide.

l are optimized to maximize the matching bandwidth for $|S_{11}| < -10$ dB or -15 dB, while other structural parameters in the1 × 4-element subarray remain unchanged. As summarized in Fig. 5 (a), the matching bandwidths for $|S_{11}| < -10$ dB and -15 dB improve with the increase of w and reach their maximum values around $w = 3.9$ mm. Since the excessively enlarged slot width may lead to the degradation in XPD, $w = 3.6$ mm is a suitable value and is adopted in the subsequent designs. On the other hand, the matching bandwidths for $|S_{11}| < -10$ dB and -15 dB also improve moderately with the increase of feeding waveguide height b, as shown in Fig. 5 (b). However, those matching bandwidths are maximized around $b = 10$ mm and degraded for larger values. Hence, $b = 10.16$ mm which is the height of the standard waveguide WR-90, is appropriate to be adopted in the subsequent designs as well.

IV. WIDEBAND DESIGN OF 1 × 4 RADIATING SLOTS

In the radiating part, the 1 × 4-element subarray of radiating slots is designed in a similar manner by applying the overload technique. Two types of boundary conditions are assumed in their external region for comparison. One is the radiation boundary condition to simulate the radiation in a half-free space; the other is the periodic boundary condition to simulate the mutual couplings in an infinite 2-D array. Introducing open-cavity as the decoupling structure is investigated as well.

A. RADIATION BOUNDARIES

As illustrated in Fig. 3 (b), since a 1-D array is under investigation, radiation boundaries are assumed in the external region. As shown in Fig. 1 (b), the longitudinal slot is offset from the waveguide axis, and the distance between the slot center and the axis is defined as slot offset p. The design procedures for achieving the matched and overloaded 1 × 4-element subarrays of radiating slots are detailed as follows.

Firstly, a single longitudinal slot with an equivalent admittance g of 1/4 is designed. According to the relationship of $g = -2S_{11}/(1 + S_{11})$, the reflection S_{11} for a single element is calculated as $-1/9$. Then, the corresponding values of $|S_{11}| = -19.5$ dB and $\angle S_{11} = 180°$ are realized by optimizing the slot offset p and length l. According to the previous studies, those two structural parameters mainly determine the amplitude and phase of S_{11}, respectively. They are optimized using HFSS and are achieved as the initial values in the subarray design.

Secondly, the structural parameters of a single slot optimized in the previous step are adopted as the initial values in the design of the 1 × 4-element subarray, where four slots with identical spacing are alternatively arranged on the left and right sides of the waveguide axis. Due to the week mutual couplings among those 1-D four slots, the normalized equivalent admittance of a single slot slightly deviates from 0.25, while the normalized equivalent admittance of the 1 × 4-element subarray slightly deviates from 1 as well. Fortunately, the matched subarray with a single resonance can be achieved as long as we fine-tune the parameters of slot offset p and length l.

Thirdly, when the slot offset value is further enlarged and the slot length is accordingly fine-tuned, a phenomenon of double resonance is observed in the frequency characteristics of the subarray's reflection.

Three types of 1 × 4-element subarrays are designed for comparison. Design requirements for impedance matching remain unchanged. They are, the worst values of $|S_{11}|$ at the center frequency are set at -10, -15, and -20 dB, respectively. As listed in Table 2, the parameters of p and l are mainly optimized to satisfy different design criteria. As the design results, the simulated reflections of those three subarrays are summarized in Fig. 6 for comparison. The matching bandwidths for $|S_{11}| < -10$, -15, and -20 dB are achieved as 17.4%, 12.2% and 8.5%, respectively. This time, by increasing the offset p, the slotted radiating waveguide is overloaded, and the matching bandwidth is enhanced. By the way, compared to the matched subarray with a single resonance, the matching bandwidth for $|S_{11}| < -15$ dB is improved by 3.6%.

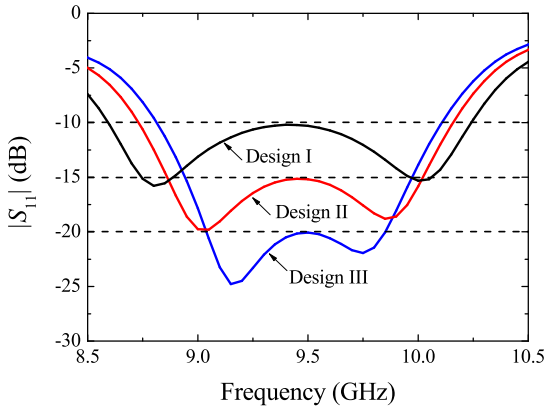

FIGURE 6. Reflection coefficient $|S_{11}|$ of 1 × 4 radiating slots for different designs under radiation boundary condition.

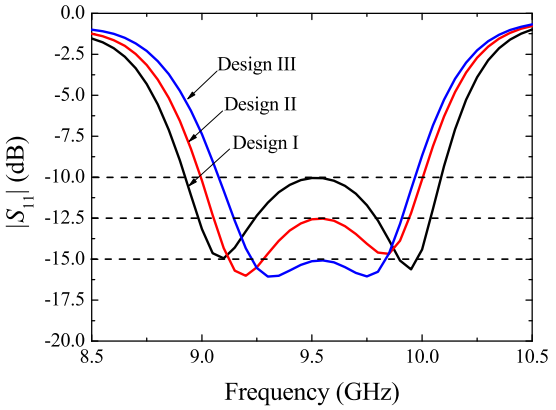

FIGURE 8. Reflection coefficient $|S_{11}|$ of 1 × 4 radiating slots for different designs under *E* & *H*-plane periodic boundary without open-cavities.

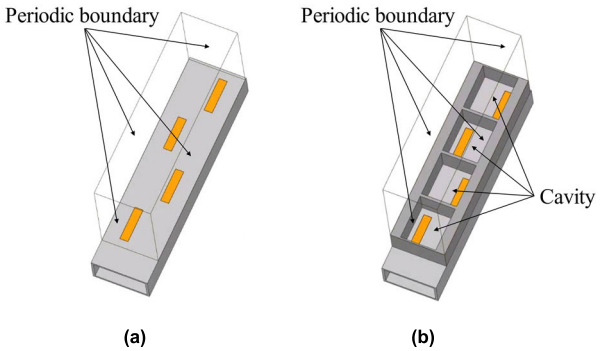

FIGURE 7. Simulation models of radiating part under periodic boundary condition. (a) Without open-cavities. (b) With open-cavities.

TABLE 2. Slot parameters and bandwidths of 1 × 4 radiating slots for different designs under radiation boundary condition.

Design	I	II	III
Max $\|S_{11}\|$ (dB)	-10	-15	-20
Slot length l (mm)	15.46	15.26	15.15
Slot offset p (mm)	4.93	4.25	3.92
Matching Bandwidth (%)	17.4	12.2	8.5

B. PERIODIC BOUNDARIES WITHOUT OPEN-CAVITIES

A 2-D array with the mutual couplings taken into account is under investigation. When simulating in HFSS, two pairs of periodic boundaries are assumed in the external region of a subarray, as illustrated in Fig. 7 (a).

The previous design procedures are re-examined here. At the center frequency, the single slot with an equivalent admittance of 0.25, and the matched subarray with a normalized input impedance of 1 are achieved in order. After that, the overload technique is applied to widen the matching bandwidth. The parameters of slot offset p and length l are optimized and summarized in Table 3. As the design results, the simulated reflections are summarized in Fig. 8 for

TABLE 3. Slot parameters and bandwidths of 1 × 4 radiating slots for different designs under *E* & *H*-plane periodic boundary without open-cavities.

Design	I	II	III
Max $\|S_{11}\|$ (dB)	-10	-12.5	-15
Slot length l (mm)	14.95	14.87	14.77
Slot offset p (mm)	3.37	3.06	2.85
Matching Bandwidth (%)	12.3	9.4	6.3

comparison. The matching bandwidths for $|S_{11}| < -10$, -12.5, and -15 dB are achieved as 12.3%, 9.4% and 6.3%, respectively. Due to introducing two pairs of periodic boundaries in both E- and H-planes, the matching bandwidth for $|S_{11}| < -15$ dB degrades by as large as 2.8%. Consequently, the introduction of decoupling structures becomes essential to improve the performance of impedance matching.

C. PERIODIC BOUNDARIES WITH OPEN-CAVITIES

In order to decouple the mutual couplings among slots as well as to enhance the bandwidth, we introduce a decoupling structure, ''open-cavity'' [30], on the top of every radiating slot. As illustrated in Fig. 7 (b), the open-cavity is surrounded by metal walls. It is equivalent to interlacing horizontal and vertical baffles around the slots. The introduction of open cavity narrows the beamwidth of the slot's radiation pattern and physically blocks the electromagnetic wave propagation close to the ground plane.

Firstly, the single slot model, where two pairs of periodic boundaries are assumed in its external region, is investigated. At the center frequency, the three dimensions of the open-cavity are optimized to achieve the active-admittance of a slot lying in a 2-D array identical to the self-admittance of the same slot lying in a half-free space, while the slot structural parameters remain unchanged. It should be noted that introducing identical cavities for all slots may function

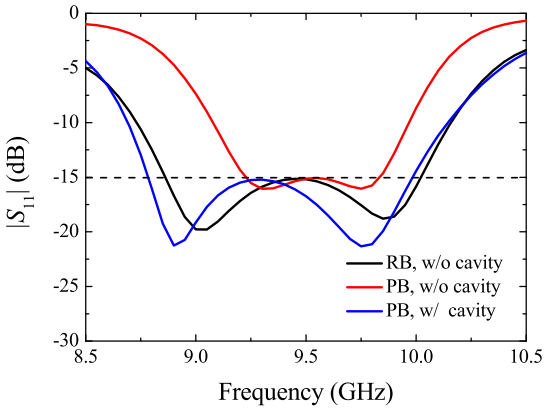

FIGURE 9. Reflection coefficient $|S_{11}|$ of 1 × 4 radiating slots for different designs.

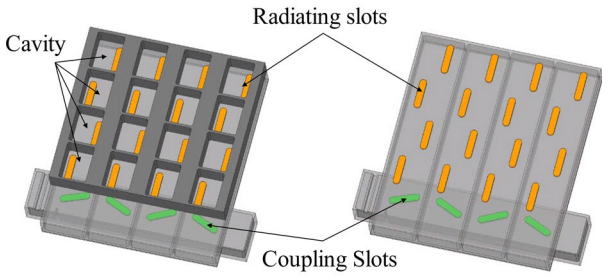

FIGURE 10. Simulation models of 4 × 4-element arrays with and without open-cavities.

well since the open-cavity effectively decouples the mutual couplings among the slots in a 2-D array.

Secondly, the optimized open-cavity is adopted in the 1 × 4-element subarray as illustrated in Fig. 7 (b), where two pairs of periodic boundaries are reserved in HFSS simulation. The parameters of slot offset p and length l listed in Table 3 are adopted as the initial values and are further fine-tuned. The structural parameters of slot are summarized in Table 4. Meanwhile, the three dimensions of the open-cavity are fine-tuned as well to maximize the matching bandwidth and the dimensions of the open-cavity is 21.04 mm × 16.08 mm × 11 mm. The reflections of 1 × 4-element subarrays with and without open-cavities are reproduced in Fig. 9 for better comprehension. According to introducing open-cavities, the matching bandwidth for $|S_{11}| < -15$ dB recovers to 12.6%, which is superior to that of the 1 × 4-element subarray adopting radiation boundaries. It follows that, when the three dimensions of the open-cavity are appropriately designed, the cavity-loaded radiating slots lying in a 2-D array operate equivalently to those slots radiate directly into the half-free space. In other words, the open-cavity effectively decouples the mutual couplings among radiating slots and further enhances the bandwidth to some extent.

V. WIDEBAND DESIGN OF 4 × 4-ELEMENT ARRAYS

The wideband designs of 1 × 4-element subarrays of both coupling and radiating slots have been investigated in detail. By applying the overload technique, wideband 1 × 4-element

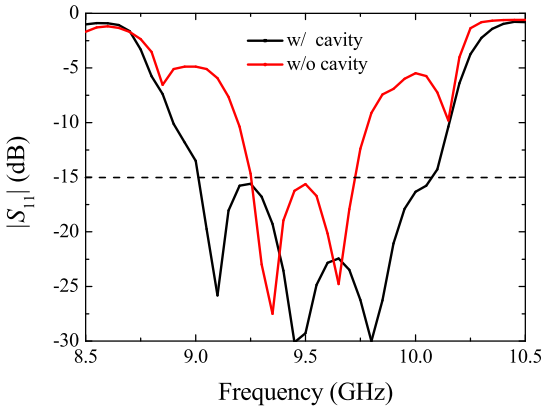

FIGURE 11. Reflection coefficient $|S_{11}|$ of 4 × 4-element subarrays with periodic boundaries.

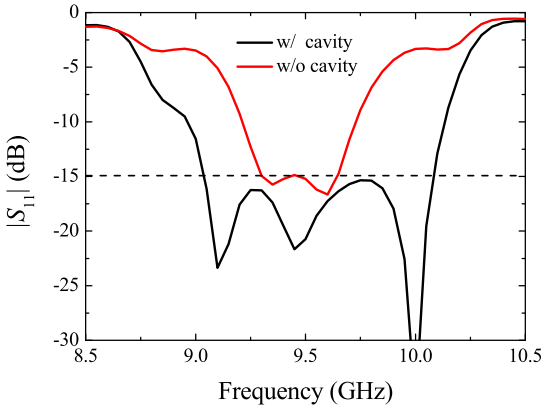

FIGURE 12. Reflection coefficient $|S_{11}|$ of 4 × 4-element arrays with radiation boundaries.

subarrays have been successfully achieved. After that, a 4 × 4-element array is under development and is constructed by combining the abovementioned 1 × 4-element subarrays. As discussed in other literature, the infinite array model associated with the periodic boundary conditions is appropriate for realizing a 2-D array with a number of elements larger than 8 × 8. However, especially in a small 2-D array, the mutual coupling effect becomes more critical, since the different element lying in different locations suffers from various mutual coupling effects. Hence, the design of a small 2-D array becomes more challenging [15]. It is worth noting that the decoupling structure may play a more crucial role in realizing a small 2-D array. Besides, the applicability of the overload technique needs further examination in such a small 2-D array. The end-fed 4 × 4-element arrays with and without open-cavities are illustrated in Fig. 10. Here, both radiation boundaries and periodic boundaries are assumed in the external regions to examine the effectiveness of both overload technique and decoupling structure.

Firstly, the periodic boundaries are assumed in the external region of the 4 × 4-element subarrays with and without cavities, which are to be adopted in a large 2-D array. As the initial parameters, the corresponding 1 × 4-element

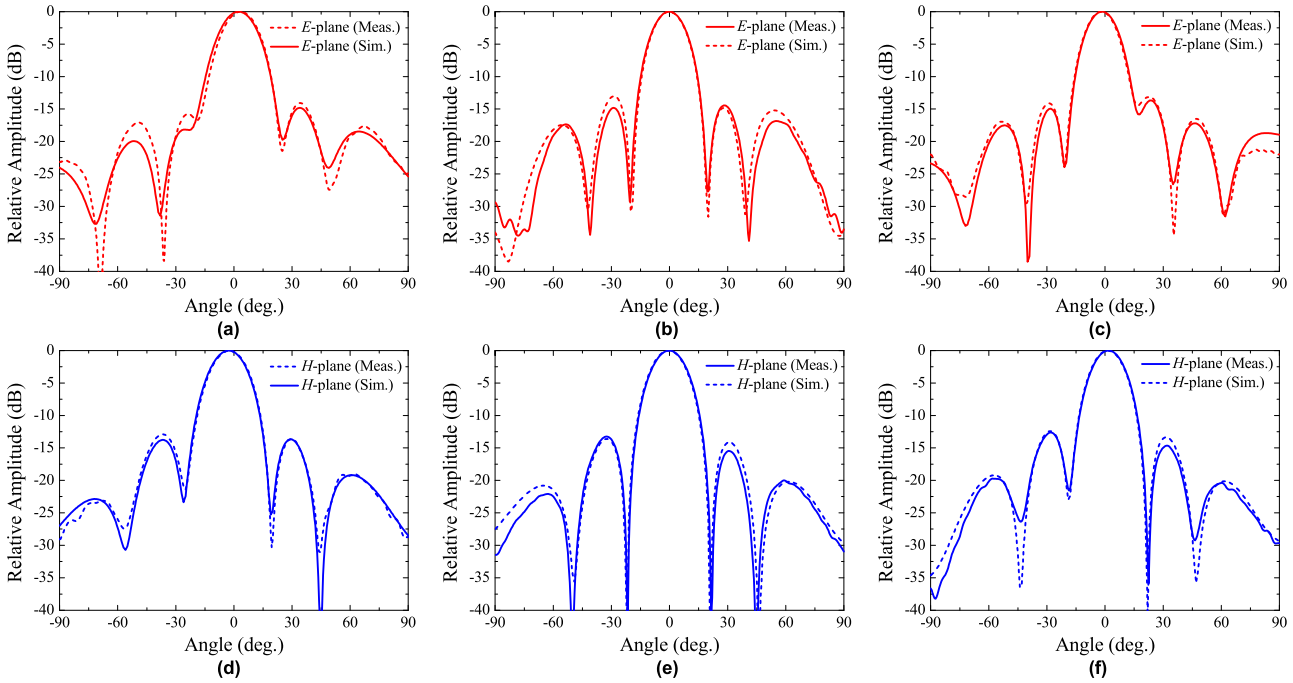

FIGURE 13. Measured and simulated radiation patterns for the 4 × 4-element array under radiation boundary in *E*-and *H*-planes. (a) *E*-plane at 9.1 GHz. (b) *E*-plane at 9.5 GHz. (c) *E*-plane at 9.9 GHz. (d) *H*-plane at 9.1 GHz. (e) *H*-plane at 9.5 GHz. (f) *H*-plane at 9.9 GHz.

TABLE 4. Slot parameters and bandwidths of 1 × 4 radiating slots for different designs.

Conditions	Slot length l (mm)	Slot offset p (mm)	BW. (%) for $\|S_{11}\| \leq$ -15 dB
RB, w/o cavity	15.26	4.25	12.2
PB, w/o cavity	14.77	2.85	9.4
PB, w/ cavity	15.12	4.18	12.6

subarrays of both coupling and radiating slots designed above are combined together. Their parameters are fine-tuned again using HFSS. By applying the overload technique, the 4 × 4-element subarrays with and without cavities are optimized for wideband operation. The frequency characteristics of their reflections are summarized in Fig. 11 for comparison. The matching bandwidth for $|S_{11}| < -15$ dB is only 5.1% for the 4 × 4-element subarray without cavities. On the other hand, the corresponding bandwidth is enhanced to 11.3% when loading open-cavities above the 4 × 4-element subarray. The phenomenon of triple resonance is achieved by fine-tuning the resonant frequencies of feeding and radiating subarrays. It is evident that the open-cavities effectively decouple the mutual couplings in the 4 × 4-element subarray, assuming the periodic boundary condition.

Secondly, the small 4 × 4-element arrays with and without cavities are designed for wideband operation. This time, radiation boundaries are assumed in the external region. Similar design procedures illustrated above are re-followed, and the structural parameters of both coupling and radiating slots are fine-tuned in HFSS. The reflections of the 4 × 4-element arrays with and without cavities are summarized in Fig. 12 for comparison. The matching bandwidth for $|S_{11}| < -15$ dB is as small as 3.8% for the 4 × 4-element array without cavities, and the corresponding bandwidth is enhanced to 11.1%, when loading open-cavities above the 4 × 4-element array. Therefore, the decoupling effect of open-cavities is remarkable and appropriate for designing small arrays. Meanwhile, the matching bandwidth of 11.1% for the array under the radiation boundary condition is comparable with that of 11.3% for the subarray under the periodic boundary condition. It is verified from another perspective that the open-cavities do effectively decouple the mutual couplings in either small or large 2-D arrays.

Moreover, the simulated field distributions over the array aperture are examined as well. According to introducing the open-cavities, the uniformities in both amplitude and phase distributions are improved significantly. A wideband cavity-loaded 4 × 4-element array with uniform aperture distribution is achieved in terms of not only impedance matching but also radiation patterns.

In consideration of antenna measurement, the transition from an SMA connector to the standard waveguide WR-90 is designed using HFSS. The cavity-loaded 4 × 4-element array fed through an SMA connector is also analyzed by HFSS. The radiation patterns in both *E*- and *H*-planes are summarized in Fig. 13. At the center frequency, the main-beams in both *E*- and *H*-planes point in the boresight direction. The first sidelobe levels are

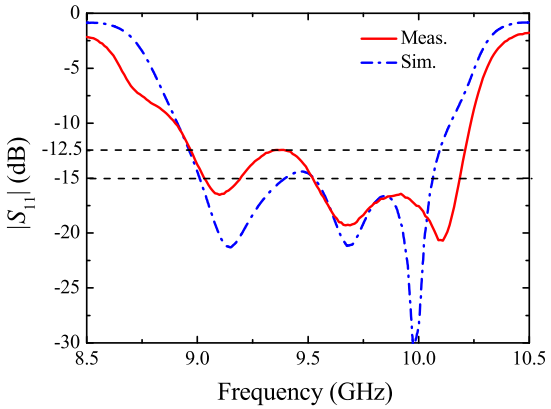

FIGURE 14. Measured and simulated reflection coefficient $|S_{11}|$ of 4 × 4-element array.

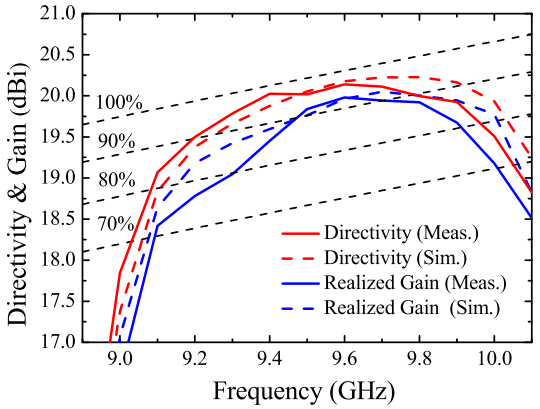

FIGURE 15. Measured and simulated directivity and realized gain of 4 × 4-element array.

-12.5 dB and -13.0 dB in the E- and H-planes, respectively. It follows that a uniform excitation is achieved. The half-power beamwidths are 16.9 and 18.5 degrees in the E-plane and H-planes, respectively. Due to the end-feed configuration as well as the long-line effect, the main-beams may slightly tilt from the boresight when the operating frequency deviates from the center frequency. The simulated antenna reflection is shown in Fig. 14. The matching bandwidth for $|S_{11}| < -15$ dB is as large as 11.1%. The simulated directivity and realized gain are summarized in Fig. 15. The bandwidth for the antenna efficiency higher than 70% is about 10.4%. Hence, the designed 4 × 4-element array behaves in wideband manners in terms of impedance matching, radiation patterns, directivity, and realized gain.

VI. FABRICATION & MEASUREMENT

Finally, the designed antenna is fabricated and measured. The 3-D printing technology has attracted considerable attention in recent years because of its low cost, flexibility, and rapid prototyping. The test antenna is fabricated by direct metal laser sintering (DMLS), which synthesizes metallic parts from metal alloy powder. It is characterized by the advantages of directly manufacturing metal and complex components with a wide selection of metal materials. At present, the DMLS technique has been successfully applied to fabricating waveguide slot arrays [31]–[34]. The antenna efficiency as high as 80% can be achieved in the microwave band, and it may degrade to some extent in the millimeter-wave band. The photograph of the test antenna fabricated by DMLS of the aluminum alloy powder is shown in Fig. 16, where the antenna dimensions are also included. The processing cycle time and cost are respectively about one week and 150 US dollars. The antenna is fed by a coaxial cable through a SMA connector designed above.

The measured and simulated radiation patterns in both E- and H-planes are included in Fig. 13 for comparison. As a wideband design, the performance of sidelobe levels in both E- and H-planes are very stable. A relatively good agreement between the simulated and measured results is observed. The

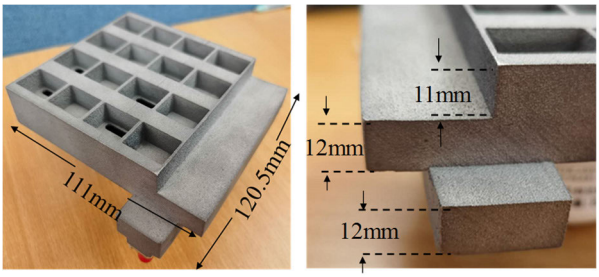

FIGURE 16. Photographs of the test antenna.

measured reflection is included in Fig. 14 for comparison. The envelopes for both measured and simulated reflections are similar to each other, while their resonant frequencies are close to each other. A small discrepancy may be caused by fine-tuning the inner conductor length during the experiment. The measured reflection degrades at the frequency of about 9.4 GHz. The matching bandwidth for the overall measured reflection below -12.5 dB is about 12.4%. The measured directivity and realized gain are included in Fig. 15 for comparison. The measured maximum aperture efficiency of 96.2% with the corresponding directivity of 20.1 dB is achieved at the frequency of 9.6 GHz. The measured maximum antenna efficiency of 92.8% with the corresponding realized gain of 20.0 dB is also achieved at the frequency of 9.6 GHz. A slight frequency shift is observed in Fig. 15. Due to our investigation, it is mainly due to machining errors. The bandwidth for the antenna efficiency higher than 70% is about 9.5%. By the way, the conductivity and the surface roughness for the test antenna contribute to the higher measured conductor loss compared with the simulated one in HFSS, where the material of pure aluminum is assumed. Consequently, we achieve the wideband 4 × 4-element array applicable in the wideband SAR and wireless communication systems. Higher antenna gain can be easily implemented by combining the 4 × 4-element subarray with a partially corporate feeding circuit.

Recently, a radial line slot array (RLSA) antenna based on the non-uniform radial TEM waveguide achieved a 3-dB gain bandwidth of as high as 27.6% [35]. The introduction of non-uniformity in the waveguiding structure plays a key role, and may provide us with an opportunity to enhance the array bandwidth further.

VII. CONCLUSION

Two techniques have been introduced in the wideband design of series-fed waveguide slot arrays. The overload technique is adopted first in the standing-wave fed 1 × 4-element arrays of both coupling slots and radiating slots. Their simulated bandwidths for $|S_{11}| < -15$ dB are enhanced to 8.1% and 12.2%, respectively. However, the effects of mutual couplings among radiating slots significantly degrade the bandwidth performance. The open-cavities functioning as the decoupling structures are additionally introduced above the radiating slots. The bandwidth of the 4 × 4 radiating slots under the periodic boundary condition successfully recovers from 5.1% to 11.3%. For demonstration, a 4 × 4-element array is designed in the X-band, and is fabricated by Direct Metal Laser Sintering technique. The measured bandwidths for $|S_{11}| < -12.5$ dB and for the antenna efficiency higher than 70% are as wide as 12.4% and 9.5%, respectively. The validity of those wideband design techniques is verified.

REFERENCES

[1] M. Hamadallah, "Frequency limitations on broad-band performance of shunt slot arrays," *IEEE Trans. Antennas Propag.*, vol. 37, no. 7, pp. 817–823, Jul. 1989.

[2] J. C. Coetzee, J. Joubert, and W. L. Tan, "Frequency performance enhancement of resonant slotted waveguide arrays through the use of wideband radiators or subarraying," *Microw. Opt. Technol. Lett.*, vol. 22, no. 1, pp. 35–39, Jul. 1999.

[3] Y. Xiaole, N. Daning, L. Shaodong, L. Zhengjun, and W. Wutu, "Design of a wideband waveguide slot array antenna and its decoupling method for synthetic aperture radar," in *Proc. Eur. Microw. Conf.*, Oct. 2008, pp. 135–138.

[4] M. Ando, Y. Tsunemitsu, M. Zhang, J. Hirokawa, and S. Fujii, "Reduction of long line effects in single-layer slotted waveguide arrays with an embedded partially corporate feed," *IEEE Trans. Antennas Propag.*, vol. 58, no. 7, pp. 2275–2280, Jul. 2010.

[5] S. R. Rengarajan and S. Chatterjee, "An investigation of bandwidth characteristics of waveguide-fed planar slot arrays," *Electromagnetics*, vol. 29, no. 7, pp. 515–521, Sep. 2009.

[6] S. R. Rengarajan and S. Chatterjee, "Bandwidth characteristics of waveguide-fed planar slot arrays," presented at the URSI Gen. Assem., Chicago, IL, USA, Aug. 2008.

[7] S. R. Rengarajan, "Coupling between waveguide-fed planar slot arrays," *IEEE Antennas Wireless Propag. Lett.*, vol. 8, pp. 429–432, Apr. 2009.

[8] S. R. Rengarajan, M. S. Zawadzki, and R. E. Hodges, "Design, analysis, and development of a large Ka-band slot array for digital beamforming application," *IEEE Trans. Antennas Propag.*, vol. 57, no. 10, pp. 3103–3109, Oct. 2009.

[9] S. R. Rengarajan, M. S. Zawadzki, and R. E. Hodges, "Waveguide-slot array antenna designs for low-average-sidelobe specifications," *IEEE Antennas Propag. Mag.*, vol. 52, no. 6, pp. 89–98, Dec. 2010.

[10] M. Zhang, J. Hirokawa, and M. Ando, "Design of a partially-corporate feed double-layer slotted waveguide array antenna in 39 GHz band and fabrication by diffusion bonding of laminated thin metal plates," *IEICE Trans. Commun.*, vol. E93-B, no. 10, pp. 2538–2544, 2010.

[11] S. Sekretarov and D. M. Vavriv, "A wideband slotted waveguide antenna array for SAR systems," *Prog. Electromagn. Res. M*, vol. 11, pp. 165–176, Jan. 2010.

[12] M. Zhang, J. Hirokawa, and M. Ando, "An E-band partially corporate feed uniform slot array with laminated quasi double-layer waveguide and virtual PMC terminations," *IEEE Trans. Antennas Propag.*, vol. 59, no. 5, pp. 1521–1527, May 2011.

[13] M. Zhang, J. Hirokawa, and M. Ando, "Double-layer plate-laminated waveguide slot array antennas for a 39 GHz band fixed wireless access system," *IEICE Trans. Commun.*, vol. E97.B, no. 1, pp. 122–128, 2014.

[14] Y. Miura, J. Hirokawa, M. Ando, Y. Shibuya, and G. Yoshida, "Double-layer full-corporate-feed hollow-waveguide slot array antenna in the 60-GHz band," *IEEE Trans. Antennas Propag.*, vol. 59, no. 8, pp. 2844–2851, Aug. 2011.

[15] D. Kim, J. Hirokawa, M. Ando, J. Takeuchi, and A. Hirata, "4 × 4-element corporate-feed waveguide slot array antenna with cavities for the 120 GHz band," *IEEE Trans. Antennas Propag.*, vol. 61, no. 12, pp. 5968–5975, Dec. 2013.

[16] D. Kim, J. Hirokawa, M. Ando, J. Takeuchi, and A. Hirata, "64 × 64-element and 32 × 32-element slot array antennas using double-layer hollow waveguide corporate-feed in the 120 GHz band," *IEEE Trans. Antennas Propag.*, vol. 62, no. 3, pp. 1507–1512, Mar. 2014.

[17] D. Kim, M. Zhang, J. Hirokawa, and M. Ando, "Design and fabrication of a dual-polarization waveguide slot array antenna with high isolation and high antenna efficiency for the 60 GHz band," *IEEE Trans. Antennas Propag.*, vol. 62, no. 6, pp. 3019–3027, Jun. 2014.

[18] Y. Wu, T. Yu, M. Zhang, D. Yu, J. Hirokawa, and Q. H. Liu, "A W-band corporate-fed hollow-waveguide slot array antenna by glass micromachining," in *Proc. Int. Symp. Antennas Propag. (ISAP)*, Jan. 2021, pp. 435–436.

[19] S. S. Yao, Y. J. Cheng, M. M. Zhou, Y. F. Wu, and Y. Fan, "D-band wideband air-filled plate array antenna with multistage impedance matching based on MEMS micromachining technology," *IEEE Trans. Antennas Propag.*, vol. 68, no. 6, pp. 4502–4511, Jun. 2020.

[20] A. Vosoogh, P.-S. Kildal, and V. Vassilev, "Wideband and high-gain corporate-fed gap waveguide slot array antenna with ETSI class II radiation pattern in V-band," *IEEE Trans. Antennas Propag.*, vol. 64, no. 4, pp. 1823–1831, Apr. 2017.

[21] D. Zarifi, A. Farahbakhsh, A. U. Zaman, and P.-S. Kildal, "Design and fabrication of a high-gain 60-GHz corrugated slot antenna array with ridge gap waveguide distribution layer," *IEEE Trans. Antennas Propag.*, vol. 64, no. 7, pp. 2905–2913, Jul. 2016.

[22] J. Liu, A. Vosoogh, A. U. Zaman, and J. Yang, "A slot array antenna with single-layered corporate-feed based on ridge gap waveguide in the 60-GHz band," *IEEE Trans. Antennas Propag.*, vol. 67, no. 3, pp. 1650–1658, Mar. 2019.

[23] Y. Li and K.-M. Luk, "60-GHz substrate integrated waveguide fed cavity-backed aperture-coupled microstrip patch antenna arrays," *IEEE Trans. Antennas Propag.*, vol. 63, no. 3, pp. 1075–1085, Mar. 2015.

[24] K. Fan, Z. Hao, Q. Yuan, G. Q. Luo, and W. Hong, "A wideband high-gain planar integrated antenna array for E-band backhaul applications," *IEEE Trans. Antennas Propag.*, vol. 68, no. 3, pp. 2138–2147, Mar. 2020.

[25] Q. Wu, J. Hirokawa, J. Yin, C. Yu, H. Wang, and W. Hong, "Millimeter-wave planar broadband circularly polarized antenna array using stacked curl elements," *IEEE Trans. Antennas Propag.*, vol. 65, no. 12, pp. 7052–7062, Dec. 2017.

[26] W. Wang, S.-S. Zhong, Y.-M. Zhang, and X.-L. Liang, "A broadband slotted ridge waveguide antenna array," *IEEE Trans. Antennas Propag.*, vol. 54, no. 8, pp. 2416–2420, Aug. 2006.

[27] S. R. Rengarajan, "Mutual coupling between waveguide-fed longitudinal broad wall slots radiating between baffles," *Electromagnetics*, vol. 16, no. 6, pp. 671–683, Nov. 1996.

[28] K. Forooraghi, P.-S. Kildal, and S. R. Rengarajan, "Admittance of an isolated waveguide-fed slot radiating between baffles using a spectrum of two-dimensional solutions," *IEEE Trans. Antennas Propag.*, vol. 41, no. 4, pp. 422–428, Apr. 1993.

[29] T. Suzuki, J. Hirokawa, and M. Ando, "Analysis and uniform design of a single-layer slotted waveguide array antenna with baffles," *IEICE Trans. Commun.*, vol. E92-B, no. 1, pp. 150–158, 2009.

[30] T. Suzuki, J. Hirokawa, and M. Ando, "Iteration-free design of waveguide slot array with cavities," *IEEE Trans. Antennas Propag.*, vol. 58, no. 12, pp. 3891–3897, Dec. 2010.

[31] S.-G. Zhou, G.-L. Huang, and T.-H. Chio, "A lightweight, wideband, dual-circular-polarized waveguide cavity array designed with direct metal laser sintering considerations," *IEEE Trans. Antennas Propag.*, vol. 66, no. 2, pp. 675–682, Feb. 2018.

[32] G.-L. Huang, S.-G. Zhou, T.-H. Chio, and T.-S. Yeo, "Fabrication of a high-efficiency waveguide antenna array via direct metal laser sintering," *IEEE Antennas Wireless Propag. Lett.*, vol. 15, pp. 622–625, 2016.
[33] G.-L. Huang, S.-G. Zhou, T.-H. Chio, C.-Y.-D. Sim, and T.-S. Yeo, "Wideband dual-polarized and dual-monopulse compact array for SAR system integration applications," *IEEE Geosci. Remote Sens. Lett.*, vol. 13, no. 8, pp. 1203–1207, Aug. 2016.
[34] Y. Wu, B. Jiang, M. Zhang, J. Hirokawa, and Q. H. Liu, "A four-corner-fed slotted waveguide sparse array for near-field focusing," *IEEE Access*, vol. 8, pp. 203048–203057, 2020.
[35] M. N. Y. Koli, M. U. Afzal, and K. P. Esselle, "Significant bandwidth enhancement of radial-line slot array antennas using a radially nonuniform TEM waveguide," *IEEE Trans. Antennas Propag.*, vol. 69, no. 6, pp. 3193–3203, Jun. 2021, doi: 10.1109/TAP.2020.3037689.

JIYU HE received the B.S. degree in electronics and information engineering from Xiamen University, Xiamen, China, in 2017, where she is currently pursuing the master's degree with the Institute of Electromagnetics and Acoustics. Her research interests include planar waveguide slot antennas and wideband antennas.

YAXIANG WU (Graduate Student Member, IEEE) received the B.S. degree in electronics and information engineering from Huaibei Normal University, Huaibei, China, in 2018. He is currently pursuing the master's degree with the Institute of Electromagnetics and Acoustics, Xiamen University, Xiamen, China.

His current research interests include waveguide slot arrays and high-gain terahertz antennas. He received the Student Paper Award at the 25th International Symposium on Antennas and Propagation (ISAP 2020), in 2021.

DAN CHEN received the B.S. degree in electronic information science and technology from Hunan Normal University, Changsha, China, in 2015, and the M.S. degree in electronics and communications engineering from Xiamen University, Xiamen, China, in 2018. Her research interest includes waveguide slot array antennas.

MIAO ZHANG (Senior Member, IEEE) received the B.S., M.S., and D.E. degrees in electrical and electronic engineering from the Tokyo Institute of Technology, Tokyo, Japan, in 2003, 2005, and 2008, respectively.

He is currently an Associate Professor with Xiamen University, Fujian, China. From 2005 to 2008, he was a Research Fellow of the Japan Society for the Promotion of Science, Tokyo. Since 2008, he has been a Researcher with the Tokyo Institute of Technology, where he became an Assistant Professor, in 2013. His research interests include waveguide slot arrays, millimeter-wave antennas, and array antennas for 5G and car-radar applications. He is a Senior Member of CIE and IEICE. He was a recipient of the Best Letter Award from the IEICE Communication Society, in 2009; the Young Engineer Award from the IEICE Technical Committee on Antennas and Propagation, in 2010; the IEEE AP-S Japan Chapter Young Engineer Award, in 2011; and the Best Paper Award at the 9th European Conference on Antennas and Propagations, in 2015.

JIRO HIROKAWA (Fellow, IEEE) received the B.S., M.S., and D.E. degrees in electrical and electronic engineering from the Tokyo Institute of Technology (Tokyo Tech), Tokyo, Japan, in 1988, 1990, and 1994, respectively.

From 1990 to 1996, he was a Research Associate with Tokyo Tech, where he was an Associate Professor, from 1996 to 2015. From 1994 to 1995, he was with the Antenna Group, Chalmers University of Technology, Gothenburg, Sweden, as a Postdoctoral Fellow. He is currently a Professor with Tokyo Tech. His research interests include slotted waveguide array antennas and millimeter-wave antennas. He is a Fellow of IEICE. He received the IEEE AP-S Tokyo Chapter Young Engineer Award, in 1991; the Young Engineer Award from IEICE, in 1996; the Tokyo Tech Award for Challenging Research, in 2003; the Young Scientists' Prize from the Ministry of Education, Culture, Sports, Science and Technology, Japan, in 2005; the Best Paper Award, in 2007; the Best Letter Award from the IEICE Communications Society, in 2009; and the IEICE Best Paper Award, in 2016 and 2018.

QINGHUO LIU (Fellow, IEEE) received the B.S. and M.S. degrees in physics from Xiamen University, Xiamen, China, and the Ph.D. degree in electrical engineering from the University of Illinois at Urbana–Champaign, Champaign, IL, USA.

From September 1986 to December 1988, he was a Research Assistant with the Electromagnetics Laboratory, University of Illinois at Urbana–Champaign, where he was a Postdoctoral Research Associate, from January 1989 to February 1990. From 1990 to 1995, he was a Research Scientist and the Program Leader with the Schlumberger-Doll Research Center, Ridgefield, CT, USA. From 1996 to May 1999, he was an Associate Professor with New Mexico State University, Las Cruces, NM, USA. Since June 1999, he has been with Duke University, Durham, NC, USA, where he is currently a Professor of electrical and computer engineering. Since 2005, he has also been the Founder and the Chairman of Wave Computation Technologies Inc. His research interests include computational electromagnetics and acoustics, inverse problems, and their application in nanophotonics, geophysics, biomedical imaging, and electronic packaging. He has published widely in these areas.

Dr. Liu is a Fellow of the Acoustical Society of America, the Electromagnetics Academy, and the Optical Society of America. He received the 1996 Presidential Early Career Award for Scientists and Engineers (PECASE) from the White House, the 1996 Early Career Research Award from the Environmental Protection Agency, the 1997 CAREER Award from the National Science Foundation, the 2017 Technical Achievement Award, the 2018 Computational Electromagnetics Award from the Applied Computational Electromagnetics Society, the 2018 Harrington-Mittra Award in Computational Electromagnetics from the IEEE Antennas and Propagation Society, and the ECE Distinguished Alumni Award from the University of Illinois at Urbana-Champaign, in 2018. He has served as the Founding Editor-in-Chief for the IEEE JOURNAL ON MULTISCALE AND MULTIPHYSICS COMPUTATIONAL TECHNIQUES and an IEEE Antennas and Propagation Society Distinguished Lecturer.